ChemistrySelect

Research Article
doi.org/10.1002/slct.202403921

Chemistry Europe
European Chemical Societies Publishing

www.chemistryselect.org

Design, Synthesis, Computational Study, and Antidiabetic Evaluation of Benzoxazole Derivatives

Amol Mahajan[+],[a] Shreyash Santosh Yadav[+],[b] Jatin Malik,[a] Dhairiya Agarwal,[a] Ramesh Ambatwar,[a] Ashok Kumar Datusalia,*[b] and Gopal L. Khatik*[a]

Alpha-amylase plays a crucial role in blood glucose levels, and thus, its inhibitor can be used to control diabetes. Thus, *in vitro alpha*-amylase inhibitory activities were studied for synthesized benzoxazole compounds. The 2-amino-benzoxazoles were prepared by reacting 2-aminophenol with cyanogen bromide, which was coupled with phenoxy acetic acid derivatives (**6 a-n**). The compound **6 h** was found to be significantly active with IC_{50} values of 348.43 μg/mL against *alpha*-amylase compared to acarbose (IC_{50} = 682.54 μg/mL). The molecular docking and molecular dynamic simulation showed better affinity and stability of **6 h** at the binding site of the *alpha*-amylase protein. Further, a preliminary bioevalauation and antidiabetic study were done through *in vivo* using SD rats. The efficacy study showed a significant improvement in glucose levels, total cholesterol, triglyceride, LDL, and HDL levels in the compound **6 h** and was found to be a lead antidiabetic agent.

1. Introduction

Diabetes mellitus (DM), a chronic metabolic disease affecting the metabolism of carbohydrates, continues to be one of the world's most devastating non-communicable diseases. DM is considered an epidemic of the 21st century. It is estimated that the global prevalence of diabetes will rise from 537 million adults (aged 20–79) in 2021 to 643 million in 2030 and 783 million by 2045.[1,2] Elevated blood glucose levels are typically the hallmark of metabolic disease. There are two main types of diabetes: type 1 and type 2.[3,4] Patients with type 1 diabetes exhibit a deficiency in insulin secretion, while type 2 diabetes can be caused by insulin resistance and a dysfunctional insulin secretory pathway.[5–7] Diabetes can have significant health implications if not properly managed and can lead to complications affecting various organs and systems, including the heart, blood vessels, eyes, kidneys, and nerves. These complications can include cardiovascular disease, diabetic retinopathy, diabetic neuropathy, kidney disease, and foot ulcers.[6,8] Many of the approaches that are being used for managing hyperglycemia in patients with type 2 diabetes involve implementing measures to impede the assimilation and absorption of carbohydrates from the diet (Figure 1).[9–14]

Alpha-amylase facilitates the enzymatic process of converting starch into glucose molecules and is present in the saliva of certain mammals, including humans. This enzyme effectively breaks down the *alpha*-(1,4) bonds of starch by hydrolysis.[15] Studies have shown that *alpha*-amylase inhibitors can effectively control postprandial (after-meal) glucose levels. They have been found to reduce the rise in blood sugar levels and improve glycemic control in individuals with type 2 diabetes. *Alpha*-amylase inhibitors are typically used as part of a comprehensive treatment plan that includes diet, exercise, and other medications.[16–19] Acarbose is a commonly used *alpha*-amylase inhibitor medication for this purpose,[20] but recently it has been found to have drug resistance via gut microbe.[21]

Recently, various newer *alpha*-amylase inhibitors were identified as small molecules like indole,[22] benzofuran hydrazine,[23] thiadiazole,[24] thiazole,[25–27] and chromone,[28] benzoxazole-based sulphonamide derivatives,[29,30] benzoxazolyl-linked benzylidene-based rhodanine and their cyclic analogues (Figure 2).[31] *Alpha*-amylase inhibitors may have adverse effects like diarrhea, flatulence, and discomfort in the abdomen are common,[32] thus new drug discovery is utmost required. We designed our target molecules by synthesising benzoxazole phenoxy acetamide as presented in Figure 2.

2. Results & Discussion

2.1. Synthesis

A solution of phenols (**1 a-h**) in water was added to sodium hydroxide pellets and reacted with chloroacetic acid (**2**) to yield the phenoxy acetic acids (**3 a-g**) (Scheme 1). 2-Amino phenols (**4 a-b**) treated with a cold suspension of cyanogen bromide under basic conditions to get 2-amino benzoxazoles (**5 a-b**). The benzoxazole phenoxy acetamide synthesis was done by an

[a] A. Mahajan,[+] J. Malik, D. Agarwal, R. Ambatwar, G. L. Khatik
Department of Medicinal Chemistry, National Institute of Pharmaceutical Education and Research Raebareli, Transit Campus, Bijnor-Sisendi Road, Sarojini Nagar, Near CRPF Base Camp, Lucknow, Uttar Pradesh, India 226002
E-mail: gopal_niper@rediffmail.com
gopal.khatik@niperraebareli.edu.in

[b] S. S. Yadav,[+] A. K. Datusalia
Department of Pharmacology & Toxicology, National Institute of Pharmaceutical Education and Research Raebareli, Transit Campus, Bijnor-Sisendi Road, Sarojini Nagar, Near CRPF Base Camp, Lucknow, Uttar Pradesh, India 226002
E-mail: ashokdatusalia@gmail.com

[+] Authors have equal contribution.

Supporting information for this article is available on the WWW under https://doi.org/10.1002/slct.202403921

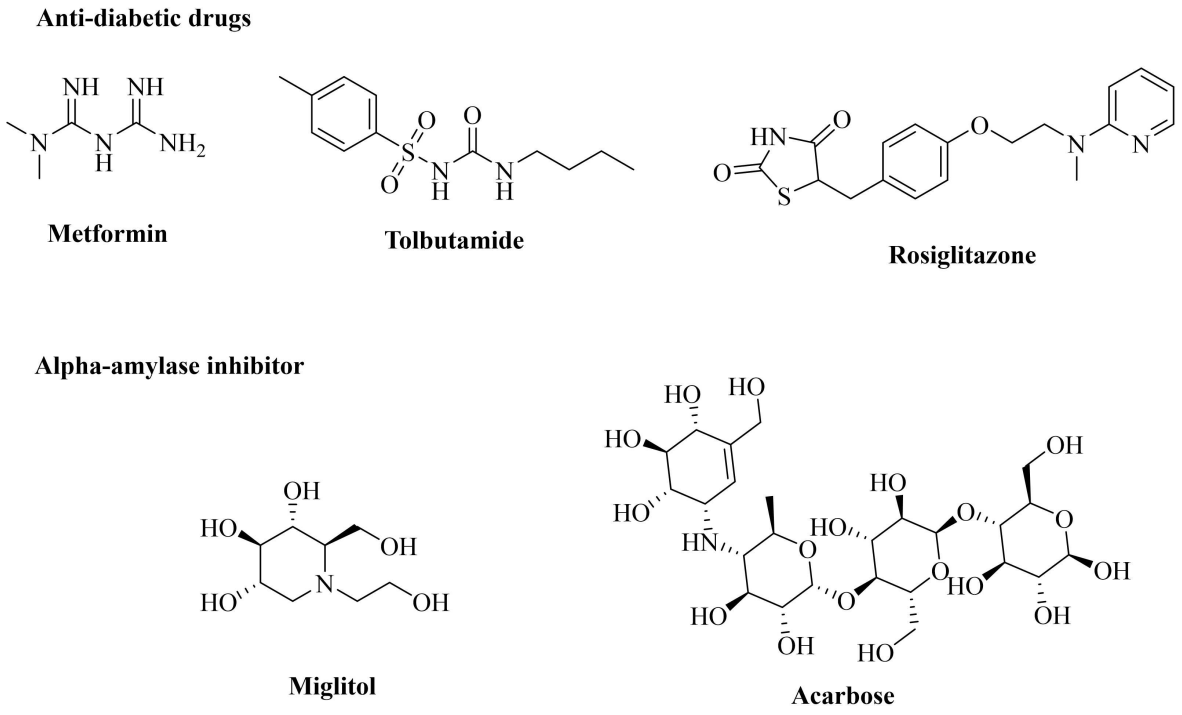

Figure 1. FDA-approved antidiabetic drugs.

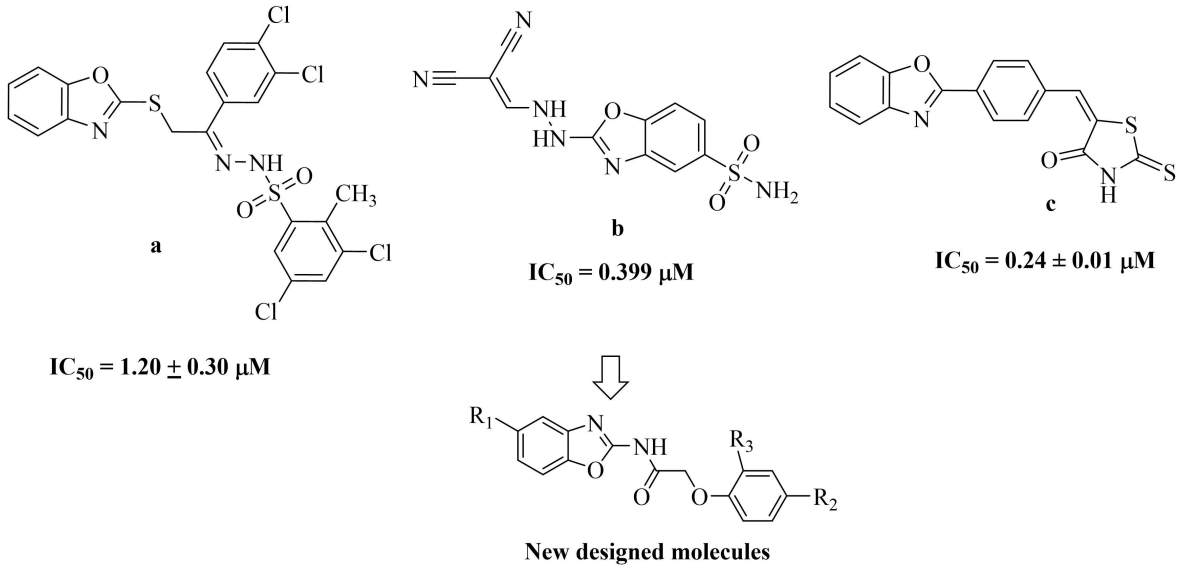

Figure 2. Benzoxazole containing potent *alpha*-amylase inhibitors and design.

amide coupling reaction between amino benzoxazoles (**5 a-b**) and phenoxy acetic acids (**3 a-h**). The coupling reaction was carried out in the presence of coupling reagent EDC.HCl (1-ethyl-3-(3-dimethylaminopropyl) carbodiimide hydrochloride) to afford benzoxazole-2-yl)-2-phenoxyacetamide derivatives (**6 a-n**).

2.2. *In vitro Alpha*-amylase Inhibitory Activity

The synthesized benzoxazole-2-yl)-2-phenoxyacetamide derivatives (**6 a-n**) were tested for their *alpha*-amylase inhibitory activity as described by Sudha *et al.*,[33] and others.[34,35] Most of the compounds were active in the micromolar range (2810.51–348.43 μg/mL). It was observed that all of them found active inhibitors of *alpha*-amylase enzyme at different extents. Some are better than acarbose (Tables 1 and S1, and Figure 3). Among these **6 h** has shown the highest activity against *alpha*-amylase

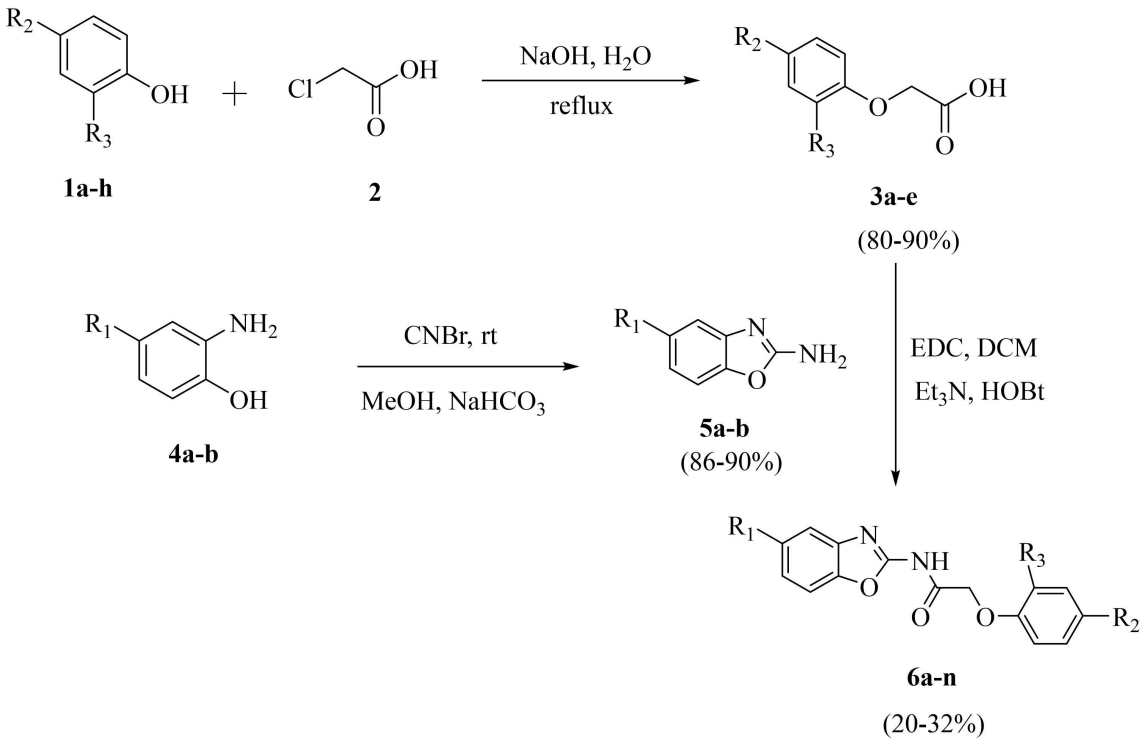

Scheme 1. Synthesis of benzoxazole-2-yl)-2-phenoxyacetamide derivatives.

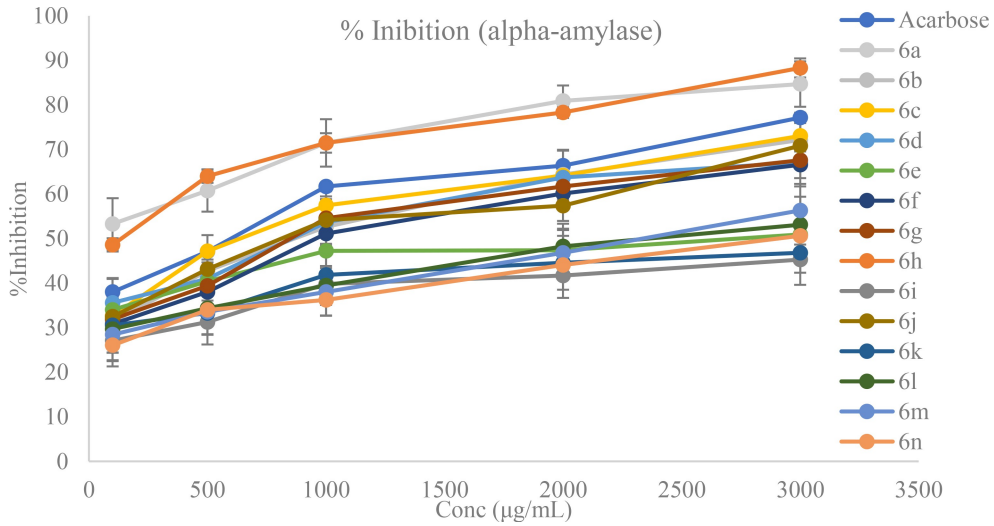

Figure 3. % inhibition of *alpha*-amylase enzyme by benzoxazole-2-yl)-2-phenoxyacetamide derivatives and acarbose at different concentrations.

enzyme with IC_{50} 348.43 µg/mL whereas **6a** was the second most potent *alpha*-amylase inhibitor with IC_{50} 566.08 µg/mL. Both were found better than the acarbose which had IC_{50} 682.54 µg/mL. These results suggested that substitution on all benzoxazole and phenyl ring has variant effects, particularly unsubstituted or Cl substitution, which led to increased alpha-amylase inhibition potency.

2.3. Structure-Activity Relationship Studies

Based on the data presented in Table 1, all compounds were evaluated for alpha-amylase inhibition activity. Compound **6h**, which has a Cl substituent on the benzoxazole ring, exhibited the most potent activity. Compound **6a**, which lacks any substitution, demonstrated the second most potent activity (Figure 4). Various substituents were tested at position R_2, including H, Cl, F, Br, and CH_3. Among these, substitution with a 4-Cl group at R_2 showed superior activity compared to the F, Br, and CH_3 derivatives. Substitution with 2-CH_3 and 2-Br groups

Table 1. IC_{50} values obtained by *alpha*-amylase inhibition.

S. No.	benzoxazole-2-yl)-2-phenoxyacetamide derivatives	Compound Code	IC_{50} (μg/mL) *Alpha*-amylase inhibition	Docking score
1	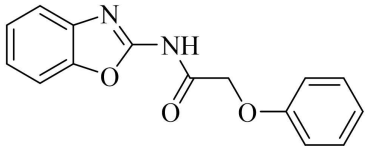	**6a**	566.08	18.62
2	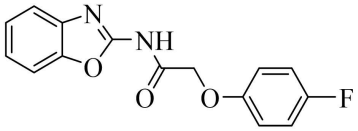	**6b**	1121.19	13.72
3	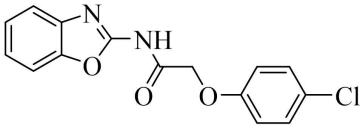	**6c**	929.84	13.83
4	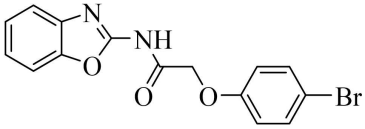	**6d**	1118.66	20.11
5	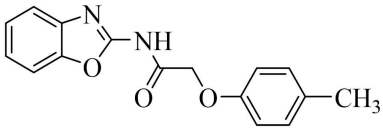	**6e**	2482.75	23.55
6	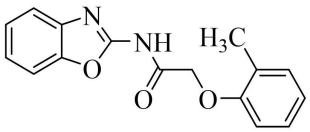	**6f**	1372.38	24.51
7	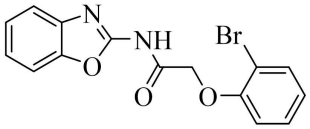	**6g**	1238.08	19.10
8	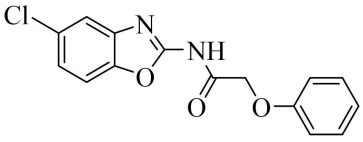	**6h**	348.43	28.35
9	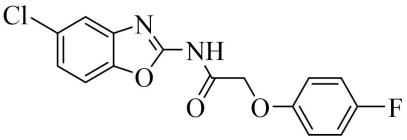	**6i**	3524.75	20.96
10	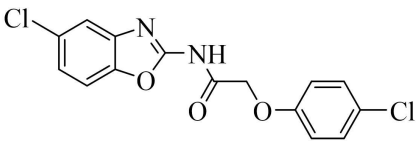	**6j**	1190.25	15.18
11	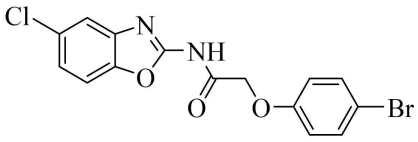	**6k**	3208.39	10.16

Table 1. continued

S. No.	benzoxazole-2-yl)-2-phenoxyacetamide derivatives	Compound Code	IC_{50} (μg/mL) *Alpha*-amylase inhibition	Docking score
12	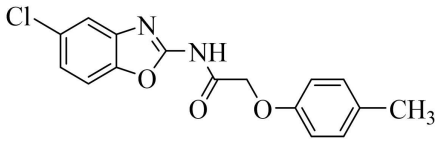	**6 l**	2434.44	21.82
13	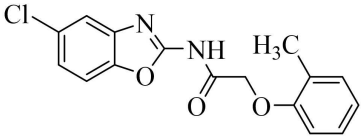	**6 m**	2313.94	24.08
14	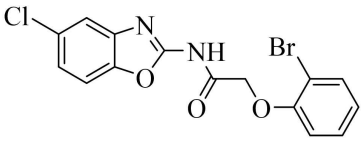	**6 n**	2810.51	33.27
15	–	Acarbose	682.54	65.91

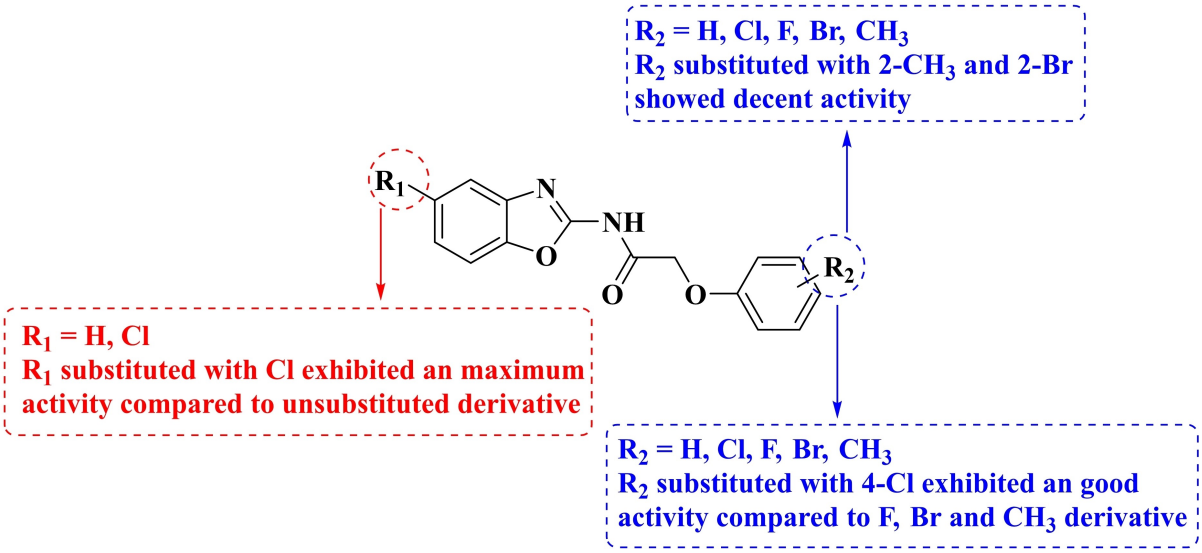

Figure 4. Proposed structure-activity relationship (SAR) of benzoxazole-2-yl)-2-phenoxyacetamide derivatives as antidiabetic agents.

also resulted in noticeable activity. The less potent activity observed with F, Br, and CH_3 could be due to less favorable interactions with the enzyme or weaker binding affinity.

2.4. Molecular Docking and Dynamic Simulation Study

All ligands were docked in the active site of *alpha*-amylase (PDB Id: 2QV4) with different docking scores using Biovia DS 2021. From the docking scores, we observed that the compounds **6 h**, and **6 n** exhibit the highest scores while **6 h** was found to be well correlated with significant interaction in active site of *alpha*-amylase and **6 a** seems to appear better in the vitro study than molecular docking study. Biovia visualizer was used to understand the type of interactions of the ligands and the co-crystallized internal ligand (Acarbose). The results were well endorsed the *in vitro alpha*-amylase inhibitory activity of compound **6 h**, and comparable to acarbose.

The 3D and 2D docking interactions of acarbose at the active site of *alpha*-amylase are shown in Figure 5. The following amino acids of chain A of *alpha*-amylase were found to interact with acarbose i.e., Asp147, Thr163, Trp59, Asp300, Arg195, Asp197, Glu233, His305, Gln63, and Gly164. Acarbose displayed conventional hydrogen bond interaction with Asp147, Asp197, Glu233, Gln63, Pi-donor hydrogen with Thr163, Trp59, Asp300, Agr195, His305, Gly164.

The 3D and 2D docking interactions of the most potent compound **6 h** at the active site of *alpha*-amylase are shown in Figure 6. The following amino acids of chain A of *alpha*-amylase were found to interact with Compound **6 h** i.e., Tyr62, Trp59, and His299. Compound **6 h** displayed, Pi–Pi stacking with Trp59, Tyr62, Pi-alkyl bond with His299.

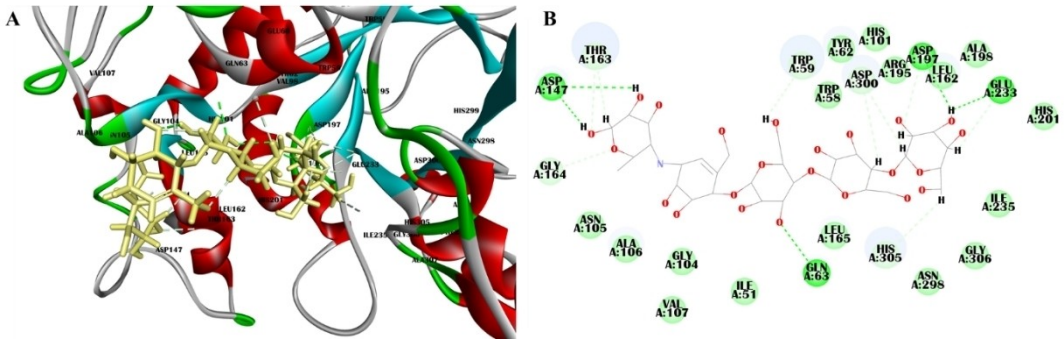

Figure 5. (A) 3D Interaction of Acarbose with *alpha*-amylase (PDB Id: 2QV4), (B) 2D interaction of acarbose with *alpha*-amylase.

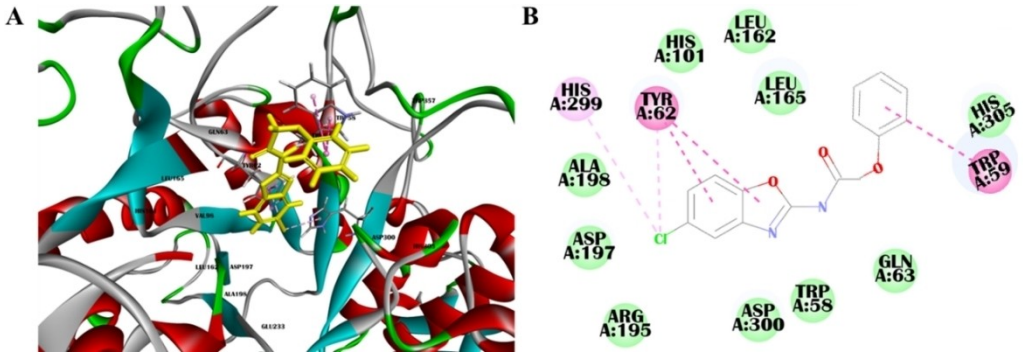

Figure 6. Key interactions of compound **6 h** with *alpha*-amylase (PDB Id: 2QV4) 3D view (A), and 2D view (B).

Docked ligands were used in CHARMM-based molecular dynamics (MD) simulation within the active site for 50 ns. We produced random ligand conformations with a high-temperature MD, and those conformations subsequently translocated into the binding site of 2QV4 protein. Finally, the ligand postures were improved by reduction.[36,37] It was noted that the average RMSD values of free alpha-amylase protein 2QV4, acarbose-2QV4, and **6 h**-2QV4, observed to be 3.075, 3.202, and 3.257 Å respectively (Figure 7A). The **6 h**-2QV4 complexes were considered stable as the RMSD values of the unbound 2QV4 and acarbose did not significantly alter. Similarly, the average RMSF values of the 2QV4, acarbose-2QV4, and **6 h**-2QV4 were 32.750, 32.752, and 32.746 Å, respectively, showing the better stability of **6 h** complex. The degree of compactness was demonstrated by the radius of gyration (Rg) graph (Figure 7B), which ranged between 33.364, 23.833, and 23.800 Å depending on the average values of the free 2QV4, acarbose-2QV4, and 6h–2QV4 docked complex. Overall, the data pointed to the creation of a stable, acarbose-like 6h–2QV4 docked complex.

2.5. *In vivo* Bioevaluation

2.5.1. Preliminary Study

From molecular docking study and *in vitro* *alpha*-amylase inhibition, we shortlisted two compounds **6 a** and **6 h** for initial *in vivo* effect on healthy SD rats. Compounds **6 a** and **6 h** were orally administered at 5 mg/kg and 10 mg/kg doses for one week. Blood was collected after the end of the treatment

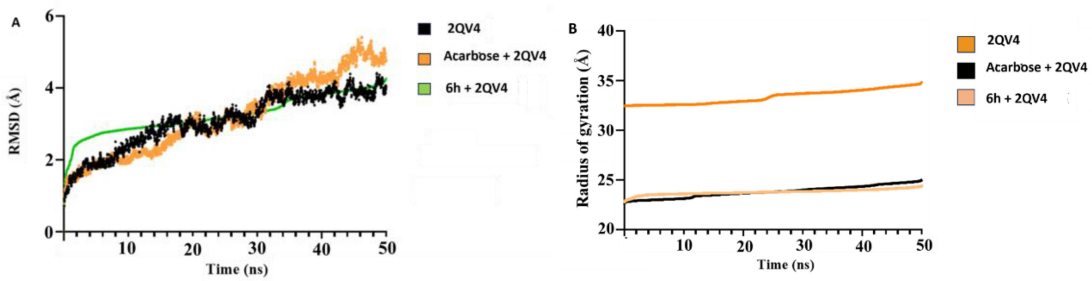

Figure 7. Molecular dynamic simulation study of free protein (6QV4), acarbose and **6 h** complex with RMSD (A), and radius of gyration (B).

period, and different blood parameters like plasma glucose levels, starch tolerance test, and lipid profiling i.e. Total cholesterol, triglyceride, LDL–C, HDL–C were performed (Figure 8A–F). In rats, the fasting plasma glucose range is 3.95 mmol/L or 71.1 mg/dL. We observed that **6a** treatment did not significantly affect the plasma glucose level. In contrast, a significant decrease in plasma glucose level was seen with 6 h treatment ($p < 0.05$) i.e. up to 80 mg/dL was seen when compared to the normal control group (Figure 8A). The glucose levels in the starch tolerance test were elevated initially till 60 min. Still, the **6a** treatment couldn't return the elevated glucose levels to normal in 120 min. while **6h** was able to return the glucose level as previously (Figure 8F). The **6a** and **6h** treatment groups didn't show any significant effect on the total cholesterol levels as well as the HDL–C levels (Figure 8B and E respectively). Furthermore, **6a** was unable to decrease the triglyceride and LDL–C levels, while **6h** ($p < 0.05$) significantly reduced their levels (Figure 8C and D). Animals were sacrificed, and gross observations were made during the necropsy for any possible sign of toxicity by **6a** and **6h** administration. The kidney sections were observed to have a normal architecture [Figure S43(A), Supplementary Information]. Further, the liver tissues were isolated and examined for tissue architecture, indicating the presence of epithelioid tumour-like cells in the case of **6a** treatment [Figure S43(B), Supplementary Information]. The results suggested that **6a** treatment showed gross signs of hepatic tissue outgrowth, whereas other organs were found to be normal. However, compound **6h** did not show any sign of toxicity in gross examination and, therefore, was selected for further *in vivo* efficacy study.

2.5.2. In vivo *Antidiabetic Study*

The body weight of all the animals was monitored daily and showed significant weight gain compared ($p < 0.001$) to the control group (Figure 9A). The plasma glucose levels in the diabetic control group (HFD + STZ) were found to be significantly increased ($p < 0.05$) compared to the control group, indicating the induction of diabetes in animals, The compound **6h** exhibited a dose-dependent effect in reducing the blood glucose levels (Figure 9B). The treatment of **6h** at a low dose of 5 mg/kg ($p < 0.05$) lowered the blood glucose levels to 78.73 mg/dL. Similarly, a high dose (10 mg/kg) showed a

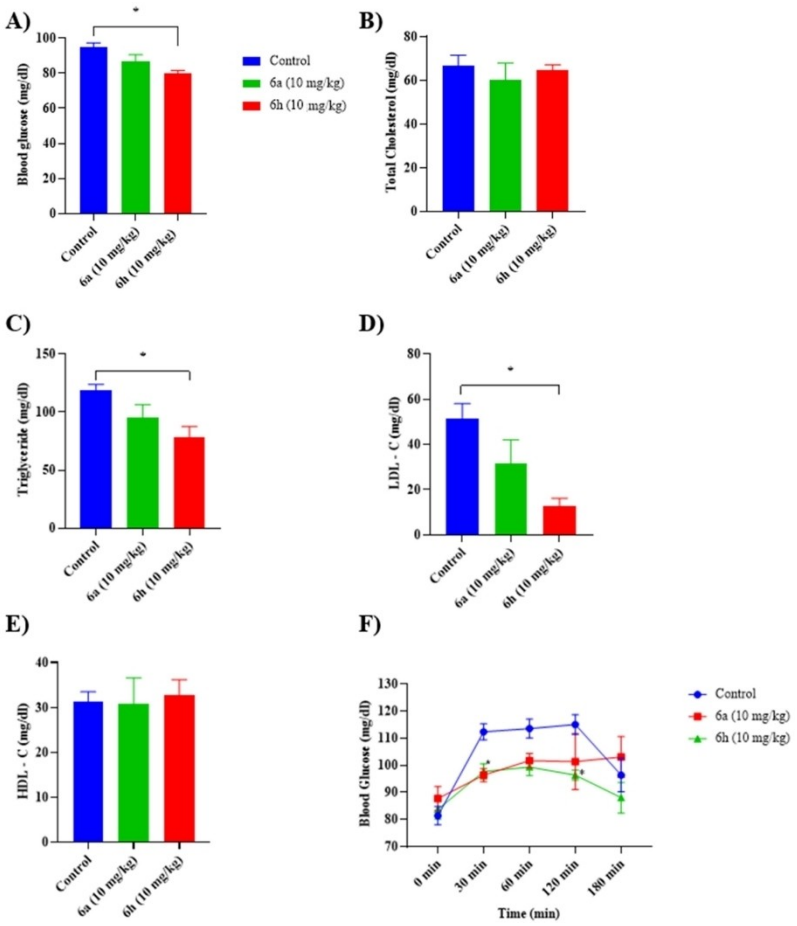

Figure 8. Evaluation of biochemical parameters after administration of test compounds **6a** and **6h**. A) Blood glucose level, B) Total Cholesterol, C) Triglyceride, D) LDL–C, E) HDL–C, F) Oral Starch Tolerance Test (OSTT), Values are reported as mean ± SEM ($n = 3–6$), Data (A–E) were analysed by using one-way ANOVA followed by Tukey's post hoc multiple comparison tests, Data (F) was analysed by using Two-way ANOVA followed by Dunnet's post hoc multiple comparison test., *$p < 0.05$, when compared with Control group.

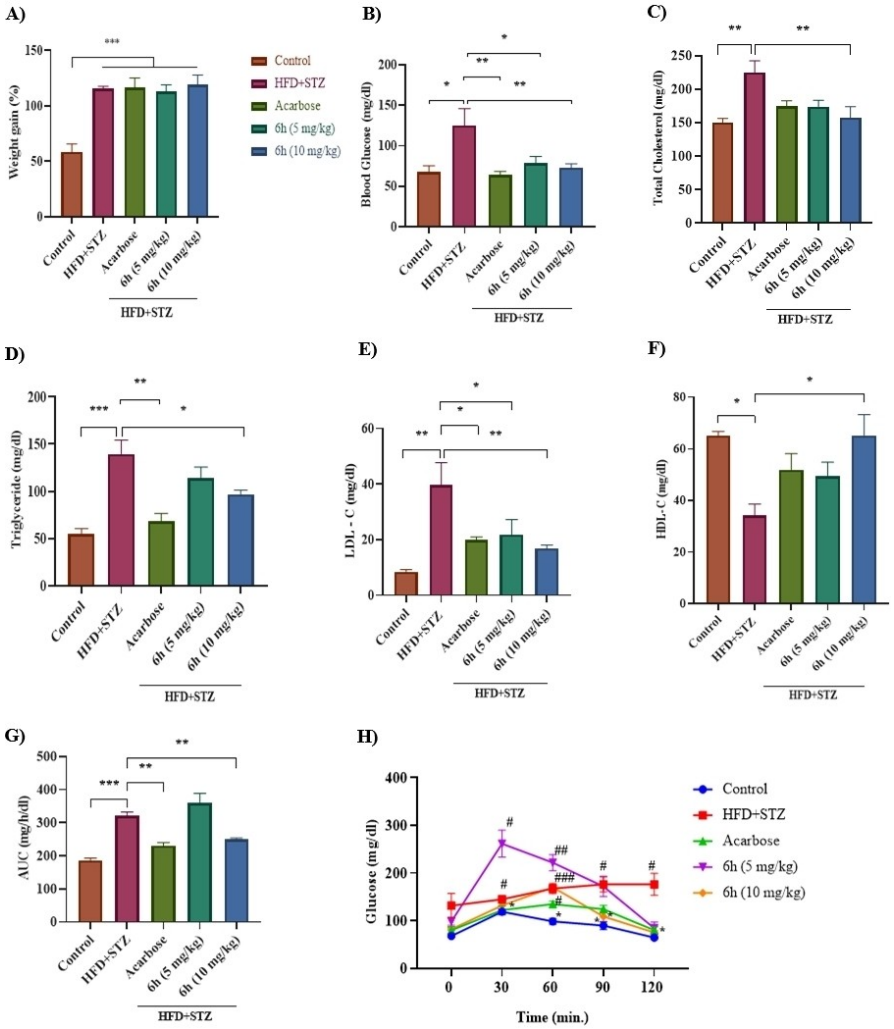

Figure 9. Evaluation of the *in vivo* efficacy and the effect on biochemical parameters with **6 h** treatment. A) Body weight (% weight gain), B) Blood glucose levels, C) Total cholesterol, D)Triglyceride, E) LDL–C, F) HDL–C, G) glucose AUC of OSTT, H) Oral Starch Tolerance Test (OSTT) Values are represented as mean ± SEM (n = 4–7), Data (A–G) were analyzed by using one-way ANOVA followed Tukey's post hoc multiple comparison test, Data (H) was analyzed by using Two-way ANOVA followed Dunnet's post hoc multiple comparison test $^{\#}p < 0.05$, $^{\#\#}p < 0.01$, $^{\#\#\#}p < 0.001$ when compared with control group, $^{*}p < 0.05$, $^{**}p < 0.01$ $^{***}p < 0.001$ when compared with diabetic control group (HFD + STZ). HFD: High Fat Diet, STZ: Streptozotocin

significant reduction ($p < 0.01$) in blood glucose level to 73.15 mg/dL, which is comparable to control animals, whereas the glucose level was also reduced significantly by the treatment with acarbose ($p < 0.01$) (a positive control). On starch loading in OSTT, a significant reduction in plasma glucose levels was seen in the control group as well in **6 h** at 10 gm/kg dose and acarbose but not as effective at 5 mg/kg dose (Figure 9H). Within 30 min, a significant decrease ($p < 0.001$) in glucose AUC (area under the curve) in the normal control groups when compared to the diabetic group (HFD + STZ) was seen. The test compound **6 h** (10 mg/kg) significantly decreased ($p < 0.01$) glucose AUC levels as compared to diabetic control and were like acarbose treated group ($p < 0.01$), demonstrating that the potential of **6 h** in effectively controlling the glucose level. The glucose AUC at 5 mg/kg dose of **6 h** showed a higher AUC at 30 min like the diabetic control group (HFD + STZ), indicating slow activity at a low dose (Figure 9G).

Total cholesterol (Figure 9C) in the diabetic control group (HFD + STZ) significantly increased compared to the normal control group. A treatment with **6 h** at 10 mg/kg led to a significant decrease ($p < 0.01$) in total cholesterol levels whereas acarbose was found to be insignificant.

The diabetic group (HFD + STZ) significantly increased ($p < 0.001$) the triglyceride levels compared to the control group (Figure 9D), whereas the acarbose and **6 h** (10 mg/kg) group showed a significant reduction at $p < 0.01$ and $p < 0.05$, respectively in the triglyceride levels when compared to STZ group. A significant increase ($p < 0.01$) in LDL level (Figure 9E) in the diabetic control group when compared to the control group was seen and this increase was significantly reduced by **6 h** at 10 mg/kg and acarbose group. HDL–C levels were seen (Figure 9F) to be decreased in the STZ group, which is usually found to be high in the normal control group. The HDL–C level was significantly increased ($p < 0.05$) by the treatment of **6 h**

(10 mg/kg) and acarbose, while the low dose was found to be insignificant.

Materials and Methods

Chemistry

All the chemicals and solvents were purchased from Sigma Aldrich, Spectrochem Pvt. Ltd., and Sisco Research Laboratories (SRL) Pvt. Ltd. and used without purification. The reactions were monitored using the Thin-layer Chromatography (TLC) on Merck pre-coated silica gel plates 60 F254 (0.25 mm), and the compounds were examined under a UV chamber. Silica gel of size #100-200 was used for column chromatography. JEOL RESONANCE ECZ500R was used to record ^{1}H and ^{13}C NMR spectra ($CDCl_3$ or DMSO-*d6*) at 500 MHz using TMS as an internal standard. Chemical shift values were given on a parts per million (ppm) scale and coupling in Hertz (Hz). Splitting patterns are described as singlet (s), doublet (d), triplet (t), multiplet (m), doublet of doublet (dd), and doublet of triplet (dt). The IR spectra were recorded on a BRUKER ECO-ATR Spectrometer.

General Procedure for the Preparation of Compound 2-Phenoxy Acetic Acid (3 a-h)

Phenol **1 a** (1.9 g, 21.0 mmol, 1 equiv) was added in water (7 mL). Sodium hydroxide pellets (2.5 g, 63.0 mmol, 3 equiv) were added to the mixture. Further chloroacetic acid **2** (1.9 g, 21.0 mmol, 1 equiv) was added immediately. The mixture was heated at 90 °C for 15 min in a boiling water bath monitoring with TLC (20% ethyl acetate in n-hexane). After heating, the mixture was cooled slightly and acidified using 6 N HCl. When the solid was dissolved, it was extracted with ethyl ether. The ethyl ether layer was evaporated under reduced pressure to obtain phenoxyacetic acid **3 a**. Compounds **3 b-h** were also prepared in this fashion.

2-Phenoxyacetic acid (3 a): White powder solid (88%); mp 118–120 °C; ESI-HRMS (*m/z*) calcd $C_8H_8O_3$ (M-H^+), 151.0395; found, 151.0447. All data was corroborated with the previous report.[38]

2-(4-Fluorophenoxy)acetic acid (3 b): White powder solid (82%); mp 128–132 °C; ESI-HRMS (*m/z*) calcd $C_8H_7FO_3$ (M-H^+), 169.0301; found, 169.0340. All data was corroborated with the previous report.[39]

2-(2-Bromophenoxy)acetic acid (3 c): White powder solid (80%); mp 134–138 °C; ESI-HRMS (*m/z*) calcd $C_8H_7BrO_3$ (M-H^+), 228.9501; found, 228.9510. All data was corroborated with the previous report.[40]

2-(4-Chlorophenoxy)acetic acid (3 d): White powder solid (83%); mp 138–140 °C; ESI-HRMS (*m/z*) calcd $C_8H_7ClO_3$ (M-H^+), 185.0006; found, 185.0013. All data was corroborated with the previous report.[41]

2-(p-Tolyloxy)acetic acid (3 e): White powder solid (90%); mp 138–140 °C; ESI-HRMS (*m/z*) calcd $C_9H_{10}O_3$ (M-H^+), 165.0552; found, 165.0565. All data was corroborated with the previous report.[41]

2-(o-Tolyloxy)acetic acid (3 f): White powder solid (90%); mp 136–140 °C; ESI-HRMS (*m/z*) calcd $C_9H_{10}O_3$ (M-H^+), 165.0552; found, 165.0563. All data was corroborated with the previous report.[42]

2-(4-Bromophenoxy)acetic acid (3 g)[39]: White powder solid (86%); mp 136–138 °C; ESI-HRMS (*m/z*) calcd $C_8H_7BrO_3$ (M-H^+), 228.9501; found, 228.9512. All data was corroborated with the previous report.[39]

General Procedure for the Preparation of benzoxazol-2-amine (5 a-b)

2-Amiophenol **4 a** (1 g, 9.1 mmol, 1 equiv.) was dissolved in methanol (10 mL) and cooled the solution by adding crushed ice. A cold suspension of cyanogen bromide (1.05 g, 10 mmol, 1.1 equiv.) was prepared by adding it to water, then the cool suspension was added to the reaction mixture by dropping funnel over 15 min with continued stirring at room temperature, followed by addition sodium bicarbonate (0.84 g, 10 mmol, 1.2 equiv.) in small portions to bring the pH 6.5–7.0 over 30 min. Stirring was continued for another 2 h. Thin layer chromatography was performed using 30% ethyl acetate in n-hexane to monitor the reaction. A rotary evaporator evaporated the extra solvent and washed it with water to benzoxazole-2 amine (**5 a**).

Benzoxazole-2 amine (5 a): Brown red solid (90%); mp 140–144 °C; ESI-HRMS (*m/z*) calcd $C_7H_6N_2O$ (M + H^+), 135.0558; found, 135.0562. All data was corroborated with the previous report.[43]

5-Chlorobenzo[d]oxazol-2-amine (5 b): Brown solid (86%); mp 180–182 °C; ESI-HRMS (*m/z*) calcd $C_7H_5ClN_2O$ (M + H^+), 169.0168; found, 169.0211. All data was corroborated with the previous report.[43]

Synthesis of N-(benzo[d]oxazol-2-yl) −2-phenoxyacetamide (6 a-n)

In a round bottom flask a mixture of phenoxy acetic acid **3 a** (1 g, 6.58 mmol, 1 equiv.), HOBt (0.1 g, 0.66 mmol, 0.1 equiv.), and DCM (10 mL) were cooled in an ice water bath. EDC.HCl (1.5 g, 7.89 mmol, 1.2 equiv.) was added to the reaction mixture and stirred for 40 min. Benzoxazole-2 amine **5 a** (0.88 g, 6.58 mmol, 1 equiv.) and triethylamine (1.85 mL, 13.16 mmol, 2 equiv) were added with continuous stirring at room temperature, further stirred for 3 h. The reaction was monitored using TLC with a 20% ethyl acetate in n-hexane. After the completion of the reaction, column chromatography was performed to purify compound **6 a**.

***N*-(Benzo[d]oxazol-2-yl)-2-phenoxyacetamide (6 a)**: Pale yellow solid (20%); mp 164–168 °C; IR (cm^{-1}): 3746 (NH), 2921 (CH), 1705 (CO); ^{1}H NMR (500 MHz, DMSO-d_6): δ 11.94 (s, 1H), 7.59 (d, J = 7.8 Hz, 1H), 7.56 (d, J = 7.7 Hz, 1H), 7.32–7.18 (m, 4H), 6.93 (d, *J* = 8.6 Hz, 3H), 4.96 (s, 2H); ^{13}C NMR (125 MHz, DMSO-d_6): δ 167.3, 158.2, 155.2, 148.1, 141.1, 130.0, 125.1, 124.2, 121.7, 118.8, 115.0, 110.6, 67.4; ESI-HRMS (*m/z*) calcd $C_{15}H_{12}N_2O_3$ (M + H^+), 269.0926; found, 269.0938.

***N*-(Benzo[d]oxazol-2-yl)-2-(4-fluorophenoxy)acetamide (6 b)**: Pale yellow solid (23%); mp 162–166 °C; IR (cm^{-1}): 3728 (NH), 3219 (NH), 1706 (CO), 1569 (C=C); ^{1}H NMR (500 MHz, DMSO-d_6): δ 11.93 (s, 1H), 7.58 (d, *J* = 7.5 Hz, 2H), 7.31–7.23 (m, 2H), 7.10 (d, *J* = 5.9 Hz, 2H), 6.97 (s, 2H), 4.92 (s, 2H); ^{13}C NMR (125 MHz, DMSO-d_6): δ 155.2, 154.5, 148.2, 141.1, 125.1, 124.2, 118.8, 116.4, 116.2, 110.6, 67.7; ESI-HRMS (*m/z*) calcd $C_{15}H_{11}FN_2O_3$ (M + H^+), 287.0832; found, 287.0838.

***N*-(Benzo[d]oxazol-2-yl)-2-(4-chlorophenoxy)acetamide (6 c)**: Whitish pink solid (27%); mp 168–170 °C; IR (cm^{-1}): 3775, 2920, 1705, 1571, 1241, 1028, 746; ^{1}H NMR (500 MHz, DMSO-d_6): δ 12.04 (s, 1H), 7.57 (m, 2H), 7.35–7.18 (m, 4H), 7.02–6.92 (m, 2H), 4.95 (s, 2H); ^{13}C NMR (125 MHz, DMSO-d_6): δ 157.1, 148.1, 140.9, 129.8, 125.4, 125.2, 124.3, 118.8, 116.9, 110.6, 67.5; ESI-HRMS (*m/z*) calcd $C_{15}H_{11}ClN_2O_3$ (M + H^+), 303.0536; found, 303.0539.

***N*-(Benzo[d]oxazol-2-yl)-2-(4-bromophenoxy)acetamide (6 d)**: Light orange solid (25%); mp 166–170 °C; IR (cm^{-1}): 3648 (NH), 2975 (CH), 1708 (CO), 1569 (C=C); ^{1}H NMR (500 MHz, DMSO-d_6): δ 11.95 (s, 1H), 7.57 (d, *J* = 9.6 Hz, 1H), 7.55 (d, *J* = 9.4 Hz, 1H), 7.45 (d, *J* = 9.0 Hz, 2H), 7.31–7.21 (m, 2H), 6.92 (d, *J* = 9.0 Hz, 2H), 4.95 (s, 2H); ^{13}C NMR (125 MHz, DMSO-d_6): δ 157.6, 155.3, 148.1, 141.6, 132.6,

125.1, 124.2, 118.6, 117.4, 113.1, 110.6, 67.4. ESI-HRMS (*m/z*) calcd $C_{15}H_{11}BrN_2O_3$ ($M+H^+$), 347.0031; found, 347.0032.

***N*-(Benzo[d]oxazol-2-yl)-2-(p–tolyloxy)acetamide (6e)**: Light brown solid (21%); mp 164–168 °C; IR (cm^{-1}): 3747 (NH), 2975 (CH), 2915 (CH), 1709 (CO), 1564 (C=C); ^{1}H NMR (500 MHz, DMSO-d_6): δ 11.90 (s, 1H), 7.59–7.54 (m, 2H), 7.29–7.25 (m, 2H), 7.06 (d, $J=8.4$ Hz, 2H), 6.82 (d, $J=8.5$ Hz, 2H), 4.87 (s, 2H), 2.19 (s, 3H); ^{13}C NMR (125 MHz, DMSO-d_6): δ 156.1, 130.4, 125.1, 124.2, 118.8, 114.9, 110.6, 67.3, 20.6; ESI-HRMS (*m/z*) calcd $C_{16}H_{14}N_2O_3$ ($M+H^+$), 283.1083; found, 283.1092.

***N*-(Benzo[d]oxazol-2-yl)-2-(o–tolyloxy)acetamide (6f)**: Pale yellow solid (20%); mp 164–166 °C; IR (cm^{-1}): 3742 (NH), 2979 (CH), 2919 (CH), 1698 (CO), 1572 (C=C); ^{1}H NMR (500 MHz, DMSO-d_6): δ 11.94 (s, 1H), 7.57 (dd, $J=17.5$, 7.8 Hz, 2H), 7.26 (dd, $J=15.3$, 4.2 Hz, 2H), 7.15–7.06 (m, 2H), 6.83 (dd, $J=12.9$, 7.7 Hz, 2H), 4.95 (s, 2H), 2.19 (s, 3H); ^{13}C NMR (125 MHz, DMSO-d_6): δ 167.7, 156.5, 155.4, 148.1, 131.1, 127.4, 126.6, 125.1, 124.2, 121.4, 118.7, 111.9, 110.6, 67.5, 16.6; HRMS (*m/z*) calcd $C_{16}H_{14}N_2O_3$ ($M+H^+$), 283.1083; found, 283.1086.

***N*-(Benzo[d]oxazol-2-yl)-2-(2-bromophenoxy)acetamide (6g)**: white powder solid (23%); mp 166–168 °C; IR (cm^{-1}): 3740 (NH), 2983 (CH), 1691 (C=C), 1577 (C=C); ^{1}H NMR (500 MHz, DMSO-d_6): δ 7.65–7.37 (m, 3H), 7.35–7.21 (m, 3H), 7.21(d, $J=500$ 1H), 7.01 (t, $J=$ 7.65, 2H), 5.07 (s, 2H); ^{13}C NMR (125 MHz, DMSO-d_6): δ 154.6, 133.6, 129.3, 125.1, 124.1, 123.0, 114.3, 111.3, 110.6, 68.1; ESI-HRMS (*m/z*) calcd $C_{15}H_{11}BrN_2O_3$ ($M+H^+$), 347.0031; found, 347.0029.

***N*-(5-Chlorobenzo[d]oxazol-2-yl)-2-phenoxy acetamide (6h)**: Brown solid (28%); mp 166–170 °C; IR (cm^{-1}): 3741 (NH), 2977 (CH), 1728 (CO), 1566 (C=C); ^{1}H NMR (500 MHz, DMSO-d_6): δ 12.09 (s, 1H), 7.67–7.60 (m, 2H), 7.30–7.23 (m, 3H), 6.96–6.90 (m, 3H), 4.92 (s, 2H); ^{13}C NMR (125 MHz, DMSO-d_6): δ 167.3, 158.2, 156.6, 146.9, 142.5, 130.1, 129.3, 124.1, 121.7, 118.5, 115.1, 111.9, 67.2; ESI-HRMS (*m/z*) calcd $C_{15}H_{11}ClN_2O_3$ ($M+H^+$), 303.0536; found, 303.0544.

***N*-(5-Chlorobenzo[d]oxazol-2-yl)-2-(4-fluorophenyl)acetamide (6i)**: Whitish pink solid (32%); mp 168–172 °C; IR (cm^{-1}): 3688 (NH), 2912 (CH), 1714 (CO), 1571 (C=C); ^{1}H NMR (500 MHz, DMSO-d_6): δ 12.07 (s, 1H), 7.70–7.58 (m, 2H), 7.27 (d, $J=10.7$ Hz, 1H), 7.09 (t, $J=$ 8.8 Hz, 2H), 6.96 (dd, $J=9.1$, 4.3 Hz, 2H), 4.91 (s, 2H); ^{13}C NMR (125 MHz, DMSO-d_6): 167.2, 158.3, 156.5, 156.4, 154.5, 146.9, 142.6, 129.3, 124.0, 118.5, 116.5, 116.4, 116.2, 111.9, 67.7; ESI-HRMS (*m/z*) calcd $C_{15}H_{10}ClFN_2O_3$ ($M+H^+$), 321.0442; found, 321.0443

***N*-(5-Chlorobenzo[d]oxazol-2-yl)-2-(4-chlorophenoxy)acetamide (6j)**: Brown solid (21%); mp 166–170 °C; IR (cm^{-1}): 3744 (NH), 2978 (CH), 1706 (CO), 1571 (C=C); ^{1}H NMR (500 MHz, DMSO-d_6): 12.09 (s, 1H), 7.69–7.60 (m, 2H), 7.32–7.26 (m, 3H), 6.97 (d, *J* 8.8 Hz, 2H), 4.94 (s, 2H); ^{13}C NMR (125 MHz, DMSO-d_6): 167.08, 157.1, 156.5, 146.9, 142.6, 129.7, 129.3, 125.4, 124.0, 118.5, 116.9, 111.9, 67.4; ESI-HRMS (*m/z*) calcd $C_{15}H_{10}Cl_2N_2O_3$ ($M+H^+$), 337.0147; found, 337.0147.

***N*-(5-Chlorobenzo[d]oxazol-2-yl)-2-(4-bromophenol)acetamide (6k)**: White solid (24%); mp 170–174 °C; IR (cm^{-1}): 3852 (NH), 3743 (NH), 2976 (CH), 1703 (CO), 1569 (C=C); ^{1}H NMR (500 MHz, DMSO-d_6): 12.09 (s, 1H), 7.69–7.59 (m, 2H), 7.43 (d, $J=8.5$ Hz, 2H), 7.28 (d, $J=8.3$ Hz, 1H), 6.92 (d, $J=8.5$ Hz, 2H), 4.94 (s, 2H); ^{13}C NMR (125 MHz, DMSO-d_6): 167.3, 157.5, 156.5, 146.9, 142.6, 132.6, 129.3, 124.1, 118.5, 117.4, 113.1, 111.9, 67.3; ESI-HRMS (*m/z*) calcd $C_{15}H_{10}BrClN_2O_3$ ($M+H^+$), 380.9642; found, 380.9649.

***N*-(5-Chlorobenzo[d]oxazol-2-yl)-2-(p–tolyl oxy)acetamide (6l)**: Whitish pink solid (28%); mp 166–168 °C; IR (cm^{-1}): 3637 (NH), 2923 (CH), 1721 (CO), 1570 (C=C); ^{1}H NMR (500 MHz, DMSO-d_6): 12.04 (s, 1H), 7.70–7.58 (m, 2H), 7.27 (d, $J=8.2$ Hz, 1H), 7.05 (d, $J=7.7$ Hz, 2H), 6.82 (d, J=7.8 Hz, 2H), 4.87 (s, 2H), 2.19 (s, 3H); ^{13}C NMR (125 MHz, DMSO-d_6): 167.4, 156.5, 156.1, 146.9, 142.6, 130.4, 130.3, 129.3, 124.1, 118.5, 114.9, 111.9, 67.3, 20.5; ESI-HRMS (*m/z*) calcd $C_{16}H_{13}ClN_2O_3$ ($M+H^+$), 317.0693; found, 317.0700

***N*-(5-Chlorobenzo[d]oxazol-2-yl)-2-(o–tolyl oxy)acetamide (6m)**: Whitish pink solid (32%); mp 166–170 °C; IR (cm^{-1}): 3664 (NH), 2899 (CH), 1758 (CO), 1577 (C=C); ^{1}H NMR (500 MHz, DMSO-d_6): 12.05 (s, 1H), 7.71–7.60 (m, 2H), 7.28 (d, $J=10.7$ Hz, 1H), 7.11 (dd, $J=20.9$, 7.5 Hz, 2H), 6.83 (dd, $J=15.6$, 7.9 Hz, 2H), 4.95 (s, 2H), 2.19 (s, 3H); ^{13}C NMR (125 MHz, DMSO-d_6): δ 167.4, 156.5, 156.4, 146.9, 142.6, 131.1, 129.3, 127.4, 126.5, 124.1, 121.4, 118.57, 111.9, 67.4, 16.6; ESI-HRMS (*m/z*) calcd $C_{16}H_{13}ClN_2O_3$ ($M+H^+$), 317.0693; found, 317.0706

***N*-(5-Chlorobenzo[d]oxazol-2-yl)-2-(2-bromophenol)acetamide (6n)**: Brown solid (26%); mp 170–174 °C; IR (cm^{-1}): 3743 (NH), 2921 (CH), 1755 (CO), 1571 (C=C); ^{1}H NMR (500 MHz, DMSO-d_6): 7.63 (dd, $J=8.4$, 5.3 Hz, 2H), 7.56 (dd, $J=7.9$, 1.4 Hz, 1H), 7.28 (m, 2H), 7.02 (dd, $J=8.3$, 0.8 Hz, 1H), 6.87 (t, $J=6.7$, 1H), 5.07 (s, 2H); ^{13}C NMR (125 MHz, DMSO-d_6): 156.77, 156.7, 154.6, 147.2, 133.6, 129.3, 129.3, 124.1, 123.1, 118.3, 114.3, 111.9, 111.3, 68.00; ESI-HRMS (*m/z*) calcd $C_{15}H_{10}BrClN_2O_3$ ($M+H^+$), 380.9642; found, 380.9636

In vitro Alpha-amylase Inhibitory Activity Assay

Alpha-amylase inhibitory activity assay was done using the iodine-starch method.[33–35] Acarbose was used as a standard. The test is based on the formation of a blue complex between iodine and starch with a maximum absorbance of 580 nm. In the positive control solution, we added both *alpha*-amylase enzyme (20 μL of 0.5 mg/mL solution) and starch but not any inhibitor, so there should be 100% enzymatic activity and minimum absorbance (since an alpha-amylase enzyme degrades maximum starch). The negative control solution did not contain an *alpha*-amylase enzyme (20 μL of 0.5 mg/mL solution) and inhibitor (test compound 500 μL of 100–3000 μg/mL), but only starch solution, which upon the addition of I_2 solution, a dark green colored complex formed which has shown maximum absorbance and no enzymatic activity. Overall, the absorbance of test solutions should be between the absorbance of positive and negative control solutions and their color intensity.[33]

Enzyme activity and % inhibition were calculated using the formula below:

$$\text{Enzyme activity} = (\text{Abs. of negative control} - \text{Abs. of positive control}) - \text{Abs. of test sample} \times 100$$

$$\text{Inhibition } (\%) = 100\text{-enzyme activity}$$

Where the absorbance of the sample (test sample + *alpha*-amylase), the absorbance of negative control (no *alpha*-amylase, 0% enzymatic activity, and 100% absorbance), and the absorbance of positive control (no inhibitor, 100 enzymatic activity, and 0% absorbance).

Inhibition concentration (IC_{50}): The concentration of the drugs at which 50% inhibition occurs.

Molecular Docking and Dynamic Simulation Study

Biovia Discovery Studio (2021) software was used to study the affinity of designed and synthesized molecules. The CDOCK module of Biovia DS (2021) was used to doc the designed benzoxazole-2-yl)-2-phenoxyacetamide derivatives and target protein. Also further

the best screened molecule conformation was put through a 50 ns molecular dynamic simulation through Biovia Discovery Studio 2022, using CHARMM force field.[44,45] The receptor grid generation was made at the same coordinates as the co-crystallized internal ligand (Acarbose), which has restricting site aspects for docking. The designed molecules were prepared and minimized using a ligand preparation module. The random conformations of the designed compounds were set to a maximum of 10 conformations. The prepared ligand was then docked with the *alpha*-amylase receptor using PDB ID (2QV4) to examine the interacting amino acids at the active site of *alpha*-amylase. The CHARMm force field was applied for docking and scoring, and other docking boundaries were kept as default. Ligand-receptor minimization *in situ* during docking was performed to eliminate any ligand van der Waals conflicts in earlier scoring and to work out restricting energy. The 5000 stages of SD with the free development of iotas inside the limiting site circle were utilized during the minimization. The binding energy of the protein-ligand complex was determined from the free energies of the complex and free energies of individual proteins and the ligand utilizing CHARMm force field and certain salvation method.

Biological Evaluation

Animals

Male Sprague Dawley (SD), weeks-old rats were procured from CSIR-Central Drug Research Institute, Lucknow, India, and were kept in the Institutional Animal House Facility. All animal husbandry procedures were maintained as per the standard operating procedures (SOPs) followed in the test facility. All experimental animals were kept in standard polypropylene cages (3 rats/cage) and maintained under controlled room temperature (22 ± 2 °C) and humidity (55 ± 5 %) with the automatically controlled cycle of 12 h light and 12 h dark. Standard laboratory animal feed and water (aqua pure) were provided ad libitum. The animals were allowed to acclimatize to experimental conditions for 1 week before the start of the experiment. Body weights and feed intake were monitored daily. All the animals were treated humanely according to the experimental protocols and standards approved by the Institutional Animal Ethics Committee (IAEC), NIPER-Raebareli (IAEC Protocol No. NIPER/RBL/IAEC/130/Dec2022).

Preliminary Study

For preliminary assessment the male SD rats were divided randomly into three different groups (n = 6): a normal control group (0.9 % saline), **6a** (10 mg/kg suspended in CMC), and 6 h (10 mg/kg suspended in CMC). The compounds **6a** and **6h** were administered for 7 days through the oral route. Blood collection was carried out by anaesthetizing the animal and puncturing the retro-orbital vein, blood was allowed to clot, and serum was separated by a cooling centrifuge set at 10,000 rpm for 10 min at 4 °C. The separated serum was kept iat at −20 °C, and later used to carry out a bioassay for Cholesterol, Triglyceride, LDL-Cholesterol, and HDl-cholesterol estimation to evaluate for any changes after the treatment. All the animals were sacrificed on the 9th day by administering urethane orally. The liver and kidneys were collected and fixed in a 10 % formalin solution for histological evaluation to check for any changes in the architecture of the tissue through Hematoxylin and Eosin (H&E) staining.

In vivo Efficacy Study

Induction of Diabetes

The animals were fed with a High Fat Diet (HFD) (contained; 60 % fat, 25 % protein, and 17 % carbohydrate, as a percentage of total kcal) *ad libitum*, for the initial period of 2 weeks, and STZ (35 mg/kg i.p) was administered on the 15th day by fasting the animals overnight. After one week of STZ administration (22nd day), Blood glucose levels were measured, and animals with fasting BGL $\geq$ 120 mg/dl were considered diabetic and further received their respective treatments after completion of 1 month of HFD.

Experimental Design

The Male SD rats were divided randomly into five different groups (n = 7):

(1) Normal control: 0.5 % CMC p.o.
(2) Disease control: HFD (60 %) + STZ (35 mg/kg, i. p.)
(3) Standard: HFD (60 %) + STZ (35 mg/kg, i. p.) + Acarbose (10 mg/kg, p.o.)
(4) Low Dose: HFD (60 %) + STZ (35 mg/kg, i. p.) + **6h** (5 mg/kg, p.o.)
(5) High Dose: HFD (60 %) + STZ (35 mg/kg, i. p.) + **6h** (10 mg/kg, p.o.)

Body weight was measured every day, along with feed intake. Glucose levels were measured before the start of the treatment. For the Starch Tolerance test animals received their respective treatment, and 10 min later, they were administered with starch suspended in distilled water at a dose of 3 g/kg of body weight orally, and blood glucose levels were measured at 0, 30, 60, 90, and 120 min after administration of respective treatment and this was conducted before sacrifice. Blood was collected and serum was separated and stored at −80 °C for evaluation of different parameters given below.

Biochemical Tests

Glucose Measurement

A glucose GOD-POD (Accurex Biomedical Pvt. Ltd.) assay kit was used to evaluate the fasting blood glucose levels. The procedure was as follows. The required amount of working reagent was prewarmed at room temperature (25–30 °C). The assay procedure was given for a total volume of 1 ml so to carry out in a microplate the volume was proportionally reduced thus 2 μL *a* plasma sample, and 200 μL of working reagents were added to the well and the assay mixture was incubated for 30 mins. at room temperature. After that absorbance was taken against blank at 505 nm.

$$\text{Glucose in mg \%} = \frac{\text{Absorbance of Sample}}{\text{Absorbance of Standard}} \times 100$$

Starch Tolerance Test

A starch tolerance test was carried out to evaluate the animal's ability to process and utilize starch and convert it into glucose. This will provide insight into the potential therapeutic effect of the treatment in a diabetic condition. As seen above 3 gm/kg of starch was used and it was administered orally 10 min after the treatment and then blood was withdrawn to check the glucose levels at different time points like 0, 30, 60, 90, and 120 mins (BG = blood

glucose at a different time in min). The AUC was calculated using the following formula:

$$AUC = \left(\frac{BG0+BG30}{2}\right)0.5 + \left(\frac{BG30+BG60}{2}\right)0.5 + \left(\frac{BG60+BG90}{2}\right)0.5 + \left(\frac{BG90+BG120}{2}\right)0.5$$

Total Cholesterol Estimation

A cholesterol (Accurex Biomedical Pvt. Ltd.) assay kit was used to evaluate the total cholesterol levels. The procedure was as follows. The required amount of working reagent was prewarmed at room temperature (25–30 °C). The assay procedure was given for total volume of 1 ml so to carry out in a microplate the volume was proportionally reduced, thus 2 μl sample and 200 μl of liquid cholesterol reagent was added to the well and the assay mixture was incubated for 10 mins. at R.T. After that absorbance was taken against blank at 510 nm.

$$\text{Conc. mg \%} = \frac{\text{Absorbance of Sample}}{\text{Absorbance of Standard}} \times 200$$

Triglyceride Estimation

The triglycerides (Accurex Biomedical Pvt. Ltd.) assay kit was used to evaluate the triglycerides levels. The procedure was as follows. The required amount of working reagent was prewarmed at room temperature (25–30 °C). The assay procedure was given for total volume of 1 ml so to carry out in a microplate the volume was proportionally reduced, thus 2 μl sample and 200 μl of liquid cholesterol reagent was added to the well and the assay mixture was incubated for 10 mins. at R.T. (25–30 °C). After that absorbance was taken against blank at 510 nm.

$$\text{Conc. mg \%} = \frac{\text{Absorbance of Sample}}{\text{Absorbance of Standard}} \times 200$$

LDL-C Estimation

To determine the levels of low-density lipoproteins (LDL) in plasma, LDL–C (Accurex Biomedical Pvt. Ltd.) assay kit was used. This was a 2-step assay in which HDL, VLDL, and Chylomicrons were eliminated by adding 2 l sample and 150 μl of Reagent 1 and incubating for 5 mins. at 37 °C and then the absorbance (A1) was measured at 546 nm, in the next step 50 μl of Reagent 2 was used to break up the LDL, this mixture was also incubated for 5 mins. at 37 °C and then the absorbance (A2) was measure at 546 nm, this made LDL-cholesterol available for measurement.

$$\text{LDL} - \text{Cholestrol in mg \%} = \frac{(\text{A2} - \text{A1})\ \text{sample}}{(\text{A2} - \text{A1})\ \text{calibrator}} \times \text{Conc. of calibrator}$$

HDL-C Estimation

To determine the levels of high-density lipoproteins (HDL) in the plasma, HDL–C (Accurex Biomedical Pvt. Ltd.) assay kit was used. This was a 2-step assay in which LDL, VLDL, and Chylomicrons were eliminated by adding 2 μL sample and 150 μL of reagent 1 and incubating for 5 mins. at 37 °C and then the absorbance (A1) was measured at 546 nm, in the next step 50 μL of Reagent 2 was used to break up the HDL, this mixture was also incubated for 5 mins. at 37 °C and then the absorbance (A2) was measured at 546 nm, this made HDL-cholesterol available for measurement.

$$\text{HDL} - \text{Cholestrol in mg \%} = \frac{(\text{A2} - \text{A1})\ \text{sample}}{(\text{A2} - \text{A1})\ \text{calibrator}} \times \text{Conc. of calibrator}$$

Statistical Analysis

Results were reported as mean ± SEM. Data was analysed by using one-way and two-way analysis of variance (ANOVA). Whenever one-way or two-way ANOVA was significant, further multiple comparisons were carried out by using Tukey's test. The level of statistical significance was adopted $P < 0.05$. The statistical analysis was done using GraphPad Prism software, version 8.0.2. (San Diego, CA, USA).

3. Conclusions

Current research focuses on finding alternative medicinal remedies with significant antidiabetic efficacy and low adverse effects. We have focused our efforts on synthesizing a series of 1-(benzoxazole-2-yl)-2-phenoxyacetamide derivatives and evaluating their antidiabetic properties. The synthesized compounds showed good inhibitory potentials targeting *alpha*-amylase. Compound **6 h** was found to be active with IC_{50} values of 348.43 μM against *alpha*-amylase agents. The molecular docking and molecular dynamic simulation showed better affinity and stability of **6 h** at the binding site of the *alpha*-amylase protein. *In vivo* data findings revealed that **6 h** was very potent in decreasing the glucose levels in the starch tolerance test and followed the same pattern as that of the control group, indicating normality after its administration. Further, significant decreases in the plasma glucose, triglyceride, total cholesterol, LDL–C level, and increase in HDL–C levels were observed. These findings reveal that 1-benzoxazole-2-yl)-2-phenoxyacetamide derivatives act as *alpha*-amylase inhibitors, which help develop novel therapeutics for treating type-II diabetes mellitus and can act as lead molecules in drug discovery as potential antidiabetic agents.

Author Contributions

AM synthesized the compounds, DA performed the *in vitro* study, and SY performed the *in vivo* study with the help of RA. JM has done the computational study. AKD and GLK hypothesized and analyzed the synthetic and biological data.

Conflict of Interests

The authors confirm that this article's content has no conflicts of interest.

Data Availability Statement

The data that support the findings of this study are available in the supplementary material of this article.

Keywords: Diabetes · *Alpha*-amylase inhibitor · Hyperglycemia · Benzoxazole · Molecular docking

[1] K. Nabrdalik, H. Kwiendacz, J. Moos, L. Moos, J. Kulpa, Z. Brzoza, T. Stompór, J. Gumprecht, G. Y. H. Lip, *Curr. Probl. Cardiol.* **2023**, *48*, 1.
[2] W. Yang, T. M. Dall, P. Halder, P. Gallo, S. L. Kowal, P. F. Hogan, M. Petersen, *Diabetes Care* **2013**, *36*, 1033.
[3] R. G. Bastos, S. O. Rodrigues, L. A. Marques, C. M. Oliveira, B. C. C. Salles, A. C. Zanatta, F. D. Rocha, W. Vilegas, J. P. Pagnossa, F. B. Fernanda, G. A. da Silva, G. E. Batiha, S. S. Aggad, B. S. Alotaibi, F. M. Yousef, M. A. da Silva, *Biomed. Pharmacother.* **2023**, *165*, 115126.
[4] P. Kaur, A. Mittal, S. K. Nayak, M. Vyas, V. Mishra, G. L. Khatik, *Curr. Drug Targets* **2018**, *19*, 1738.
[5] A. J. Radia, J. N. Lalpara, I. J. Modasiya, G. G. Dubal, *J. Heterocycl. Chem.* **2021**, *58*, 612.
[6] I. Khan, W. Rehman, F. Rahim, R. Hussain, S. Khan, L. Rasheed, M. M. Alanazi, A. S. Alanazi, M. H. Abdellattif, *ACS Omega* **2023**, *8*, 22508.
[7] Y. Hu, J. Xu, J. Wang, L. Zhu, J. Wang, Q. Zhang, *ACS Chem. Neurosci.* **2023**, *14*, 3335.
[8] D. Care, S. S. Suppl, *Diabetes Care* **2022**, *45*, 185.
[9] K. Bednarz, *Life Artic.* **2024**, *14*, 1.
[10] M. Pangrace, S. Dolan, T. Grace, E. Greene, E. Long, S. McClelland, J. Moore, D. E. Morgan, H. Mullins, S. Wescott, *J. Manage. Care Specialty Pharm.* **2024**, *30*, S1.
[11] B. E. Marks, K. M. Williams, J. S. Sherwood, M. S. Putman, *J. Clin. Transl. Endocrinol.* **2022**, *27*, 100282.
[12] J. J. Shelke, A. R. Roscoe, J. A. Morrow, G. R. Colman, L. K. Banerjee, T. K. Kirshner, P. Susan, *Bone* **2008**, *23*, 1.
[13] M. Alzyoud, R. Alazaidah, M. Aljaidi, G. Samara, M. H. Qasem, M. Khalid, N. Al-Shanableh, *Int. J. Data Netw. Sci.* **2024**, *8*, 179.
[14] K. K. Venkatesh, X. Huang, N. A. Cameron, L. C. Petito, J. Joseph, M. B. Landon, W. A. Grobman, S. S. Khan, *BJOG An Int. J. Obstet. Gynaecol.* **2024**, *131*, 26.
[15] L. Gong, D. Feng, T. Wang, Y. Ren, Y. Liu, J. Wang, *Food Sci. Nutr.* **2020**, *8*, 6320.
[16] S. S. Hamdani, B. A. Khan, M. N. Ahmed, S. Hameed, K. Akhter, K. Ayub, T. Mahmood, *J. Mol. Struct.* **2020**, *1200*, 127085.
[17] B. Usman, N. Sharma, S. Satija, M. Mehta, M. Vyas, G. L. Khatik, N. Khurana, P. M. Hansbro, K. Williams, K. Dua, *Curr. Pharm. Des.* **2019**, *25*, 2510.
[18] R. Bashary, M. Vyas, S. K. Nayak, A. Suttee, S. Verma, R. Narang, G. L. Khatik, *Curr. Diabetes Rev.* **2020**, *16*, 117.
[19] R. Bashary, G. L. Khatik, *Bioorg. Chem.* **2019**, *82*, 156.
[20] A. Aispuro-Pérez, J. López-Ávalos, F. García-Páez, J. Montes-Avila, L. A. Picos-Corrales, A. Ochoa-Terán, P. Bastidas, S. Montaño, L. Calderón-Zamora, U. Osuna-Martínez, J. I. Sarmiento-Sánchez, *Bioorg. Chem.* **2020**, *94*, 103491.
[21] J. Tian, C. Li, Z. Dong, Y. Yang, J. Xing, P. Yu, Y. Xin, F. Xu, L. Wang, Y. Mu, X. Guo, Q. Sun, G. Zhao, Y. Gu, G. Qin, W. Jiang, *Nat. Metab.* **2023**, *5*, 896.
[22] M. Taha, M. S. Baharudin, N. H. Ismail, S. Imran, M. N. Khan, F. Rahim, M. Selvaraj, S. Chigurupati, M. Nawaz, F. Qureshi, S. Vijayabalan, *Bioorg. Chem.* **2018**, *80*, 36.
[23] M. Taha, S. A. A. Shah, S. Imran, M. Afifi, S. Chigurupati, M. Selvaraj, F. Rahim, H. Ullah, K. Zaman, S. Vijayabalan, *Bioorg. Chem.* **2017**, *75*, 78.
[24] M. Taha, M. Tariq Javid, S. Imran, M. Selvaraj, S. Chigurupati, H. Ullah, F. Rahim, F. Khan, J. Islam Mohammad, K. Mohammed Khan, *Bioorg. Chem.* **2017**, *74*, 179.
[25] G. L. Khatik, A. K. Datusalia, W. Ahsan, P. Kaur, M. Vyas, A. Mittal, S. K. Nayak, *Curr. Drug Discovery Technol.* **2018**, *15*, 163.
[26] H. Mehmood, M. Haroon, T. Akhtar, S. Woodward, S. Haq, S. M. Alshehri, *Future Med. Chem.* **2024**, *16*, 1255.
[27] M. Haroon, H. Iqbal, T. Akhtar, A. Aktaş, *Chem. Biodivers.* **2024**, *27*, e202401021.
[28] A. T. Benny, S. D. Arikkatt, C. G. Vazhappilly, S. Kannadasan, R. Thomas, M. S. N. Leelabaiamma, E. K. Radhakrishnan, P. Shanmugam, *Mini-Reviews Med. Chem.* **2021**, *22*, 1030.
[29] S. Khan, F. Rahim, W. Rehman, M. Nawaz, M. Taha, S. Fazil, R. Hussain, S. Adnan Ali Shah, M. H. Abdellatif, *Arab. J. Chem.* **2022**, *15*, 104341.
[30] M. Rodrigues, B. Bennehalli, V. H. Manjappaiah, S. Anantha, *Trends Sci.* **2021**, *18*, 35.
[31] V. Singh, A. Singh, G. Singh, R. K. Verma, R. Mall, *Med. Chem. Res.* **2018**, *27*, 735.
[32] A. Nasir, M. Khan, Z. Rehman, A. A. K. Khalil, S. Farman, N. Begum, M. Irfan, W. Sajjad, Z. Parveen, *Plants (Basel)* **2020**, *9*, 852.
[33] P. Sudha, S. S. Zinjarde, S. Y. Bhargava, A. R. Kumar, *BMC Complementary Altern. Med.* **2011**, *11*, 5.
[34] S. Hameed, Kanwal, F. Seraj, R. Rafique, S. Chigurupati, A. Wadood, A. U. Rehman, V. Venugopal, U. Salar, M. Taha, K. M. Khan, *Eur. J. Med. Chem.* **2019**, *183*, 111677.
[35] M. Devi, P. Kumar, R. Singh, J. Sindhu, R. Kataria, *Eur. J. Med. Chem.* **2023**, *250*, 115230.
[36] N. R. Jabir, M. T. Rehman, K. Alsolami, S. Shakil, T. A. Zughaibi, R. F. Alserihi, M. S. Khan, M. F. AlAjmi, S. Tabrez, *Ann. Med.* **2021**, *53*, 2332.
[37] M. Shahwan, M. S. Khan, F. M. Husain, A. Shamsi, *J. Biomol. Struct. Dyn.* **2022**, *40*, 3871.
[38] K. Anbarasu, K. K. Ilavenil, *Asian J. Chem.* **2018**, *30*, 2239.
[39] D. Yan, D. Li, G. Cheng, Z. Yang, L. Shi, D. Guo, *J. Fluoresc.* **2015**, *25*, 849.
[40] Y. H. Eissa Mohammed, P. Thirusangu, Zabiulla, V. Vigneshwaran, P. B. T. S. A. Khanum, *Biomed. Pharmacother.* **2017**, *95*, 375.
[41] H. M. Pallavi, F. H. Al-Ostoot, H. K. Vivek, S. A. Khanum, *J. Mol. Struct.* **2022**, *1247*, 131404.
[42] Y. H. E. Mohammed, V. H. Malojirao, P. Thirusangu, M. Al-Ghorbani, B. T. Prabhakar, S. A. Khanum, *Eur. J. Med. Chem.* **2018**, *143*, 1826.
[43] D. Li, C. Liu, X. Jiang, Y. Lin, J. Zhang, Y. Li, X. You, W. Jiang, M. Chen, Y. Xu, S. Si, *Eur. J. Med. Chem.* **2021**, *209*, 112898.
[44] F. Hosseini, M. Mohammadi-Khanaposhtani, H. Azizian, A. Ramazani, M. B. Tehrani, H. Nadri, B. Larijani, M. Biglar, H. Adibi, M. Mahdavi, *Struct. Chem.* **2020**, *31*, 999.
[45] J. C. Phillips, R. Braun, W. Wang, J. Gumbart, E. Tajkhorshid, E. Villa, C. Chipot, R. D. Skeel, L. Kalé, K. Schulten, *J. Comput. Chem.* **2005**, *26*, 1781.

Manuscript received: August 16, 2024